Extended Kalman Filter Design for Semilinear Distributed Parameter Systems with Application to Anaerobic Digestion

Ivan Yupanqui Tello[1,2], Alain Vande Wouwer[1]
[1]*Systems, Estimation, Control and Optimization (SECO)*
University of Mons, Mons, Belgium
ivanfrancisco.yupanquitello@umons.ac.be,
alain.vandewouwer@umons.ac.be

Daniel Coutinho[2]
[2]*Department of Automation and Systems*
Universidade Federal de Santa Catarina
Florianópolis, Brazil
daniel.coutinho@ufsc.br

***Abstract*—This paper is concerned with the online state estimation of a class of one-dimensional semilinear partial differential equation (PDE) systems considering piecewise measurements over the spatial domain. In the context of infinite-dimensional linear systems, it is well-known that the Kalman filter minimizes the mean square estimation error. For semilinear infinite-dimensional systems, the extended Kalman filter (EKF) is a widely used extension relying on successive linearizations of the estimation error dynamics. In this paper, we propose a computationally tractable implementation of the EKF using a sample-and-hold approach for which the optimal output injection operator associated to the proposed estimator is computed at each sampling time via the approximate solution of the infinite-dimensional Riccati equation. The performance of the observer is exemplified through numerical experiments which demonstrate the efficiency of the proposed approach.**

***Index Terms*—State estimation, Riccati equation, Process monitoring, Biochemical systems**

I. Introduction

Distributed biochemical reaction systems involve spatial and temporal concentration, temperature, and possibly pressure, profiles. Tubular reactors are the main example of such systems [2]. Their state variables are described by partial differential equations (PDEs) consisting of material, energy and momentum balances that couple the effects of advection, reaction, and diffusion along with initial and boundary conditions. The time and space dependencies as well as certain types of boundary conditions make the analysis of distributed reaction systems complex [3].

For process monitoring and control, the knowledge of the system states is of fundamental importance. However, there exists a number of obstacles associated with the lack of reliable sensors capable of providing on-line measurements of the state variables along the whole spatial domain, and in this case, the internal states have to be estimated from the measurement of process inputs and outputs. State observers for distributed parameter systems are usually based on a PDE model of the system together with an additional output injection term to improve the convergence of the observation error [4]. Several types of observers or filters have been proposed for tubular biochemical reactors, including moving horizon observers [5], interval observers [6], matrix inequality-based observers [7], dissipative observers [8], sliding mode observers [9], among others.

For monitoring and control purposes, the observers are numerically implemented with a computer, and there are two main options for the discretization step, either at an early stage, i.e., model discretization, or at a later stage, i.e., state observer discretization [4]. In the last decades, the state estimation of distributed-parameter systems based on the late-lumping approach has reached important milestones such as the modal design for linear and semi-linear systems [1], [8], [10]. Nonetheless, there are still some important issues concerning the design of state estimators that are feasible for online implementation, in particular, for semi-linear PDE systems with in-domain measurements. In this work, we are interested in the optimal state estimation of a particular class of distributed tubular reactor systems. Specifically, we investigate the online implementation of the extended Kalman filter (EKF) for a particular application example, e.g., a bioreactor system used in wastewater treatment with Monod type kinetics which belongs to the class of Sturm–Liouville systems (see [11] and the references therein for a definition and their connection with Riesz-spectral systems).

By exploiting spectrum properties of Sturm–Liouville operators, we propose an EKF algorithm considering a sample-and-hold approach in which the infinite-dimensional Riccati equation is converted into a set of coupled algebraic equations which are numerically solved at each sampling time.

The remainder of this paper is organized as follows. Section II states the problem of interest. In particular, an anaerobic digestion process described by a semilinear PDE system is equivalently expressed in terms of a well-posed abstract infinite-dimensional system. Section III presents the EKF algorithm for the infinite dimensional system with the output injection operator being determined from the solution of the infinite-dimensional Riccati equation. Then, a sample-

This work was partially supported by CAPES and CNPq/Brazil under grants 88881.171441/2018-01 and 302690/2018-2/PQ, respectively.

Cite as: I. F. Yupanqui Tello, D. . Coutinho, and A. Vande Wouwer, "Extended Kalman Filter Design for Semilinear Distributed Parameter Systems with Application to Anaerobic Digestion", *Syst. Theor. Control Comput. J.*, vol. 1, no. 1, pp. 95–103, Jun. 2021.
DOI: 10.52846/stccj.2021.1.1.18

and-hold based approach is introduced to computationally implement the EKF algorithm. In Section IV, the results are illustrated through numerical simulations and Section V provides some concluding remarks and points out possible future research lines.

Notation. Throughout this work, the mathematical notation is standard for infinite dimensional systems; see, e.g., [10]. Also, we denote the set of positive real numbers by $\mathbb{R}^+$, the set of positive integer numbers by $\mathbb{N}^+$, the vector space of n_x-by-n_y real matrices by $\mathbb{R}^{n_x \times n_y}$, $Q > 0$ denotes that Q is a symmetric and positive definite matrix, δ_{nm} represents the Kronecker delta function, $\partial_z x(z,t)$ and $\partial_z^2 x(z,t)$ are the first and second partial derivatives of the function $x(z,t)$, with respect to z, respectively. $\mathbf{L}_2(0,1)$ denotes the space of square Lebesgue integrable functions on the interval $(0,1)$, i.e.

$$\mathbf{L}_2(0,1) = \left\{ x : (0,1) \to \mathbb{R} : \left(\int_0^1 x^2(z) dz \right)^{\frac{1}{2}} < \infty \right\}.$$

Unless otherwise indicated, $\langle x_1, x_2 \rangle$ denotes the inner product of x_1 and x_2, with $x_1, x_2 \in \mathbf{L}_2(0,1)$. The set $L(\mathbb{R}^n, \mathbf{L}_2(0,1))$ includes bounded linear operators from $\mathbb{R}^n$ to $\mathbf{L}_2(0,1)$ endowed with the induced norm. The adjoint operator of the differential operator $\mathcal{A}$ with domain $\mathcal{D}(\mathcal{A}) \subset \mathbf{L}_2(0,1)$ is denoted by $\mathcal{A}^*$ with domain $\mathcal{D}(\mathcal{A}^*) \subset \mathbf{L}_2(0,1)$ and satisfies

$$\langle \mathcal{A} x_1, x_2 \rangle = \langle x_1, \mathcal{A}^* x_2 \rangle$$

for all $x_1 \in \mathcal{D}(\mathcal{A})$ and $x_2 \in \mathcal{D}(\mathcal{A}^*)$. The identity operator on $\mathbf{L}_2(0,1)$ is denoted by $\mathcal{I}$.

$Z_d(z)$ denotes the vector of monomial basis of degree d or less, i.e,

$$Z_d(z) = \begin{bmatrix} 1 & z & \cdots & z^{d-1} & z^d \end{bmatrix}.$$

Instrumental Results. The following definition and lemma will be instrumental to derive the main results of this paper

Definition 1: [11] Consider the differential operator defined as

$$\mathcal{A} = \frac{1}{\rho(z)} \left(\partial_z (p(z) \partial_z) - q(z) \mathcal{I} \right),$$

where the functions $p(z),\ \rho(z) \in \mathbb{R}^+$ are continuously differentiable and $q(z) \in \mathbb{R}$ is continuous on $[0,1]$. Furthermore, the domain $\mathcal{D}(\mathcal{A})$ is given by

$$\begin{aligned} D(\mathcal{A}) = \big\{ x \in \mathbf{L}_2(0,1) : x,\ \partial_z x \text{ are absolutely continuous,} \\ \partial_z^2 x \in \mathbf{L}_2(0,1) \text{ and } \alpha_0 \partial_z x(0) + \beta_0 x(0) = 0 \\ \partial_z \alpha_1 \partial_z x(1) + \beta_1 x(1) = 0 \big\}. \end{aligned}$$

where $(\alpha_0, \beta_0) \neq (0,0)$ and $(\alpha_1, \beta_1) \neq (0,0)$. Then, $-\mathcal{A}$ is said to be a Sturm-Liouville operator.

Lemma 1: [11] Any Sturm-Liouville operator is a Riesz-spectral operator.

The immediate consequence of the above result is that the properties of Riesz-spectral systems and operators [10] can be used in the analysis and control of Sturm-Liouville systems, in particular for convection-diffusion-reaction systems.

II. Problem Statement

Consider an anaerobic digestion process (used for wastewater treatment) operated in a fixed bed reactor [12], with the methanization occurring in the limiting step. Then, the process kinetics can be characterized by the following reaction scheme

$$S \to X + \text{biogas}$$

where S and X represent the substrate (organic matter to be degraded) and the biomass, respectively. In a first approximation and in line with the physical evidence, it is assumed that the biomass X varies very slowly in comparison to the substrate S, and remains almost constant. Moreover it is also assumed that X is spatially uniform.

It should be stressed that the latter assumptions are *a priori* plausible. They were introduced here in order to simplify the presentation of the proposed approach, but coupling effects can be addressed similarly to the analysis that follows. Furthermore, it is also assumed that the kinetics is described by a Monod law. Under these conditions, the process dynamics can be described (considering a dimensionless representation) by the following semi-linear parabolic equation (i.e., a diffusion–convection–reaction model):

$$\partial_t x(z,t) = \frac{1}{P_e} \partial_z^2 x(z,t) - \partial_z x(z,t) - k_0 \frac{x(z,t)}{1 + x(z,t)} \tag{1}$$

subject to the Danckwerts' boundary conditions

$$\begin{aligned} \frac{1}{P_e} \partial_z x(0,t) - x(0,t) &= -x_{in}(t) \\ \partial_z x(1,t) &= 0 \end{aligned} \tag{2}$$

where P_e is the (dimensionless) Peclet number (i.e., $P_e = \upsilon l / D_a$), and x, x_{in}, τ and z are dimensionless variables defined as follows:

$$x = \frac{S}{S_{sat}},\ x_{in} = \frac{S_{in}}{S_{sat}},\ t = \frac{\tau \upsilon}{L},\ z = \frac{\zeta}{l} \tag{3}$$

with $\upsilon,\ l,\ D_a,\ S,\ S_{sat},\ S_{in},\ \tau$ and ζ denoting the fluid superficial velocity, the reactor length, the axial diffusion coefficient, the substrate concentration, the saturation constant, the inlet substrate concentration, the time and the spatial variable, respectively. The parameter k_0 is given by

$$k_0 = \frac{\mu_{max} l X_0}{S_{sat} \upsilon Y} \tag{4}$$

where X_0, μ_{max} and Y are the assumed constant biomass, the maximum specific growth rate and the yield coefficient, respectively.

The adopted numerical values for the process parameters are taken from Table I

TABLE I
PARAMETER VALUES.

Parameter	Value	Definition
P_{eT}	5	Peclet number
k_0	0.875	Damkohler number
x_{in}	1	Inlet concentration

For numerical simulation purposes we generate the initial condition profile of $x(z,t)$ through the solution of a semidefinite programming problem formulated in (5) that can be solved by using conventional SOS (sum of squares) tools [17], i.e., the initial condition $x(0,t) = x_0(z)$ is selected as a positive polynomial satisfying the boundary conditions and with one upper bound selected by the physical conditioning of the process.

$$\begin{cases} \text{Find } x_0(z) = Z_d^T(z) Q Z_d(z), \quad Q > 0 \\ \quad \text{subject to} \\ \frac{1}{P_e}\partial_z x_0(0) - x_0(0) = -x_{in} \\ \quad \partial_z x_0(1) = 0 \\ \quad x_0(z) < 0.4. \end{cases} \tag{5}$$

We considered $d = 3$ in Problem (5) for generating an initial condition profile, then the numerical simulation has been implemented using a finite-difference discretization with $N_{nod} = 85$ nodes. The time evolution profiles of $x(z,t)$ is shown in Figure 1. It was obtained by solving numerically (1)-(2) considering the parameters given in Table I and initial condition obtained through the solution of the semidefinite programming problem in (5).

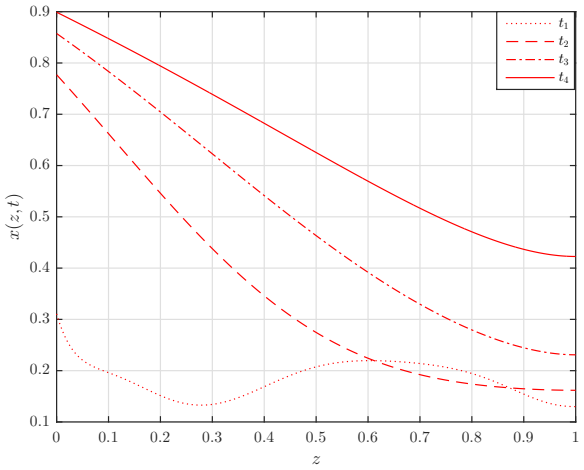

Fig. 1. Time evolution of the spatial profile of $x(z,t)$ at time instants $t_1 = 0,\ t_2 = 0.25,\ t_3 = 0.5,\ t_4 = 1$

In this paper, we are interested in estimating $x(z,t)$ from a finite number of measurements (spatially distributed). More precisely, the state estimation problem of system (1)-(2) consists in designing a dynamical observer on the basis of its mathematical model and online measurements given by

$$y(t) = \begin{bmatrix} \int_0^1 c_1(z)x(z,t)dz \\ \vdots \\ \int_0^1 c_{n_y}(z)x(z,t)dz \end{bmatrix} \in \mathbb{R}^{n_y} \tag{6}$$

where $c_j(z)$ describes the distribution of the measurement at the j-th position over the spatial domain $[0,1]$.

In practical applications, measurement sensors are only placed at a finite number of discrete points (or partial areas) of the spatial domain. The definition of functionals $c_1(z), \ldots, c_{n_y}(z)$ will characterize the local measurements. For instance, the following definition

$$c_j(z) = 1_{[z_j-\varepsilon_j, z_j+\varepsilon_j]} = \begin{cases} \frac{1}{2\varepsilon_j}, & z_j-\varepsilon_j \le z \le z_j+\varepsilon_j, \\ 0, & \text{elsewhere} \end{cases} \tag{7}$$

produces n_y zones of piecewise uniform sensing in the interval $[z_j - \varepsilon_j, z_j + \varepsilon_j]$ as illustrated in Figure 2.

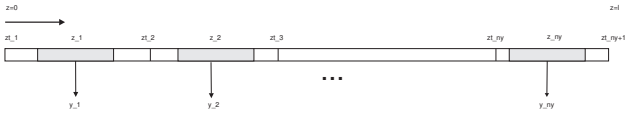

Fig. 2. Distributed piecewise measurements

.

Remark 1: Notice that $c_j(z),\ j = 1, ..., n_y$ in the above definition are elements in $\mathbf{L}_2(0,1)$ for fixed, small, positive constants $\varepsilon_j,\ j = 1, ..., n_y$. We remark that these piecewise functions define bounded output operators on the Hilbert state space. Usually, a pointwise sensor is modelled as a delta distribution at the point j, i.e., $\delta(z - z_j)$ replaces $c_j(z)$, and they may yield unbounded operators within this approach: it may maps out of the Hilbert state space $\mathbf{L}_2(0,1)$.

III. THE EXTENDED KALMAN FILTER

Consider the following equivalent state-space description of the model (1)–(2), i.e., the abstract differential equation on the Hilbert space $\mathbf{L}_2(0,1)$, (see, e.g., [10]):

$$\begin{aligned} \dot{x}(t) &= \mathcal{A}x(t) + G\ r(x(t)) \\ \mathfrak{B}x(t) &= u(t) \\ y(t) &= \mathcal{C}x(t) \end{aligned} \tag{8}$$

where $x(t) = x(\cdot,t) \in \mathbf{L}_2(0,1)$, $u(t) = [-x_{in}(t)\ \ 0]^T \in \mathbb{R}^2$ and the operators $\mathcal{A} : \mathcal{D}(\mathcal{A}) \to \mathbf{L}_2(0,1)$, $\mathfrak{B} : \mathcal{D}(\mathfrak{B}) \subset \mathcal{D}(\mathcal{A}) \to \mathbb{R}^2$, $\mathcal{C} : D(\mathcal{C}) \subset \mathcal{D}(\mathcal{A}) \to \mathbb{R}^{n_y}$ are defined as

$$\mathcal{A} = \frac{1}{P_e}\partial_z^2 - \partial_z$$

$$D(\mathcal{A}) = \{x \in \mathbf{L}_2(0,1) : x,\ \partial_z x \quad \text{are absolutely continuous}, \\ \partial_z^2 x \in \mathbf{L}_2(0,1)\} \tag{9}$$

$$\mathfrak{B}x = \begin{bmatrix} \frac{1}{P_e}\partial_z x(0) - x(0) \\ \partial_z x(1) \end{bmatrix} \tag{10}$$

$$\mathcal{C}x = \begin{bmatrix} \langle c_1, x\rangle \\ \vdots \\ \langle c_{n_y}, x\rangle \end{bmatrix}. \tag{11}$$

and $G = -k_0$ and $r(x) = \dfrac{x}{1+x}$.

The system representation (8) has to be extended to consider noisy measurements.

$$\begin{aligned} \dot{x}(t) &= \mathcal{A}x(t) + G\ r(x(t)) \\ \mathfrak{B}x(t) &= u(t) \\ y(t) &= \mathcal{C}x(t) + v(t) \end{aligned} \tag{12}$$

where it is assumed that $v(t) \in \mathbf{L}_2([0,\infty), \mathbb{R}^{n_y})$ is uncorrelated white Gaussian noise with zero mean and covariance $V > 0$.

The fundamental result for infinite-dimensional linear systems is the well-known Kalman filter [13]. Based on system representation (12), the following observer is defined

$$\begin{aligned} \dot{\hat{x}}(t) &= \mathcal{A}\hat{x}(t) + Gr\left(\hat{x}(t)\right) + \mathcal{L}(t)\left(\hat{y}(t) - y(t)\right) \\ \mathfrak{B}\hat{x}(t) &= u(t) \\ \hat{y}(t) &= \mathcal{C}\hat{x}(t) \end{aligned} \tag{13}$$

where $\mathcal{L}(t) : \mathbb{R}^+ \to L(\mathbb{R}^{n_y}, \mathbf{L}_2(0,1))$ is a time-varying output injection operator.

Now, let

$$e(t) = x(t) - \hat{x}(t) \tag{14}$$

be the state estimation error. Then, the estimation error dynamics is given by

$$\begin{aligned} \dot{e}(t) &= \left(\mathcal{A} + \mathcal{L}(t)\mathcal{C}\right)e(t) + G\left(r(x(t)) - r(\hat{x}(t))\right) \\ &\qquad + \mathcal{L}(t)v(t) \\ \mathfrak{B}e(t) &= 0. \end{aligned} \tag{15}$$

Considering the linear approximation based on Taylor series expansion around $\hat{x}(t)$, it follows that

$$r(x(t)) \cong r(\hat{x}(t)) + \partial_x r(\hat{x}(t))e(t) \tag{16}$$

which results in the (extended) linearization of (15) with respect to the reconstructed state trajectory $\hat{x}(t)$:

$$\dot{e}(t) = \left(\tilde{\mathcal{A}}(t) + \mathcal{L}(t)\mathcal{C}\right)e(t) + \mathcal{L}(t)v(t) \tag{17}$$

where

$$\begin{aligned} \tilde{\mathcal{A}}(t) &= \mathcal{A} + G\ \partial_x r\left(\hat{x}(t)\right)\mathcal{I} \\ \mathcal{D}(\tilde{\mathcal{A}}) &= \mathcal{D}(\mathcal{A}) \cap \ker\left(\mathfrak{B}\right). \end{aligned} \tag{18}$$

As in (linear) Kalman filter design [13], the output injection gain is taken as

$$\mathcal{L}(t) = -\hat{\Pi}(t)\mathcal{C}^* V^{-1} \tag{19}$$

where $\hat{\Pi}(t) : \mathbb{R}^+ \to L(\mathbf{L}_2(0,1))$ is a self adjoint non-negative operator and the unique solution of the infinite-dimensional differential Riccati equation

$$\begin{aligned} \left\langle \dot{\hat{\Pi}}(t)\xi_1, \xi_2 \right\rangle &= \left\langle \hat{\Pi}(t)\xi_1, \tilde{\mathcal{A}}^*(t)\xi_2 \right\rangle + \left\langle \tilde{\mathcal{A}}^*(t)\xi_1, \hat{\Pi}(t)\xi_2 \right\rangle \\ &\qquad - \left\langle \mathcal{C}\hat{\Pi}(t)\xi_1, V^{-1}\mathcal{C}\hat{\Pi}(t)\xi_2 \right\rangle \\ \hat{\Pi}(0) &= \hat{\Pi}_0 \end{aligned} \tag{20}$$

for all $\xi_1,\ \xi_2 \in \mathcal{D}(\tilde{\mathcal{A}}^*)$, $\forall t \geq 0$, with $V \in \mathbb{R}^{n_y \times n_y}$ being symmetric and positive definite. We emphasize that the Riccati equation (20) and the observer equation (13) in principle have to be solved simultaneously because $\tilde{\mathcal{A}}(t)$ depend on $\hat{x}(t)$.

Assumption 1: $r(\cdot) : \mathbf{L}_2(0,1) \to \mathbf{L}_2(0,1)$ has a locally Lipschitz derivative, i.e., there exists a positive constant $l^r = l^r(\rho)$ where $\rho > 0$ such that

$$\|\partial_x r(x) - \partial_x r(\hat{x})\| = l^r \|x - \hat{x}\|. \tag{21}$$

holds for all $x, \hat{x} \in \mathbf{L}_2(0,1)$ with $\|x\|, \|\hat{x}\| \leq \rho$.

Assumption 2: There exists a bounded self adjoint non-negative operator $\hat{\Pi}(t) : \mathbb{R}^+ \to L(\mathbf{L}_2(0,1))$ that is the unique solution of the infinite-dimensional differential Riccati equation (20) and subject to the observer equation (13) for all $t > 0$.

The above assumptions are crucial to ensure the well-posedness of the extended Kalman filter design problem, Although the second one is not straightforward to verify, we know from the properties of the Riccati equation that this assumption is satisfied if the pair $(\tilde{\mathcal{A}}(t), \mathcal{C})$ is uniformly observable. Since the operator $\tilde{\mathcal{A}}(t)$ is generated in real time, we cannot check their observability off line. Thus, in order to obtain a convergent solution, a successive iteration procedure which is incorporated into the extended Kalman filter framework is considered below.

A. *Sample and Hold Approach*

The computation of the output injection operator $\mathcal{L}(t)$ of the extended Kalman filter relies on the successive (extended) linearization of the semilinear error dynamics as defined in (15). As a result, the extended Kalman filter induces a large computational effort due to continuously determining the self-adjoint operator $\hat{\Pi}(t)$. Hence, in order to provide an efficient computational procedure, a sample-and-hold approach is introduced in the sequel which will allow the online implementation of the observer [14].

In order to illustrate the principle, it is assumed that the output $y(t)$ is updated only at discrete time instants t_i, $i \in \mathbb{N}$, with a constant sampling period given by

$$\Delta t = t_{i+1} - t_i.$$

Next, let $\hat{x}(t_i) = \hat{x}(\cdot, t_i)$ and compute the output injection gain $\mathcal{L}(t_i)$ at sampling instant t_i so that

$$\mathcal{L}(t) = \mathcal{L}(t_i), \quad \forall\ t \in [t_i, t_{i+1}]$$

thus, the Riccati-equation (20) is made time-invariant in the sampling intervals and has to be solved for

$$\begin{aligned} \tilde{\mathcal{A}}(t_i) = \ \tilde{\mathcal{A}}_i &= \mathcal{A} + G\ \partial_x r\left(\hat{x}(t_i)\right)\mathcal{I} \\ \mathcal{D}(\tilde{\mathcal{A}}_i) &= \mathcal{D}(\mathcal{A}) \cap \ker\left(\mathfrak{B}\right) \end{aligned} \tag{22}$$

avoiding the differentiation with respect to time, that is:

$$\begin{aligned} \left\langle \hat{\Pi}_i \xi_1, \tilde{\mathcal{A}}_i^* \xi_2 \right\rangle + \left\langle \tilde{\mathcal{A}}_i^* \xi_1, \hat{\Pi}_i \xi_2 \right\rangle \\ - \left\langle \mathcal{C}\hat{\Pi}_i \xi_1, V^{-1}\mathcal{C}\hat{\Pi}_i \xi_2 \right\rangle = 0. \end{aligned} \tag{23}$$

for all $\xi_1,\ \xi_2 \in \mathcal{D}(\tilde{\mathcal{A}}_i^*)$.

More specifically, notice that $\tilde{\mathcal{A}}_i$ is a linear time invariant operator for $t \in [t_i, t_{i+1}]$ given by

$$\tilde{\mathcal{A}}_i = \frac{1}{P_e}\partial_z^2 - \partial_z - k_i(z)\mathcal{I} \tag{24}$$

with

$$k_i(z) = \frac{k_0}{(1 + \hat{x}(z, t_i))^2}$$

and

$$\begin{aligned} &D(\tilde{\mathcal{A}}_i) = \mathcal{D}(\mathcal{A}) \cap \ker(\mathfrak{B}) \\ &D(\tilde{\mathcal{A}}_i) = \{x \in \mathbf{L}_2(0,1) : x,\ \partial_z x \ \text{ are absolutely continuous,} \\ &\qquad \partial_z^2 x \in \mathbf{L}_2(0,1) \ \text{ and } \ -\frac{1}{P_e}\partial_z x(0) + x(0) = 0 \\ &\qquad \partial_z x(1) = 0\}. \end{aligned} \tag{25}$$

Figure 3 illustrates this principle setup. Furthermore, each $\tilde{\mathcal{A}}_i$ is the negative part of a Sturm-Liouville operator, since it has the following form

$$\tilde{\mathcal{A}}_i = \frac{1}{\rho(z)}\left(\partial_z(p(z)\partial_z) - q(z)\mathcal{I}\right), \tag{26}$$

with ρ, p and q being such that

$$\begin{aligned} \rho(z) = \mathrm{e}^{-P_e z} > 0, \quad p(z) = \frac{1}{P_e}\rho(z) > 0, \\ q(z) = -k_i(z). \end{aligned} \tag{27}$$

Following the analysis in [11], [15], the spectrum of $\tilde{\mathcal{A}}_i$ consists only of real, countable and single eigenvalues. More specifically, the spectrum $\sigma(\tilde{\mathcal{A}}_i)$ of $\tilde{\mathcal{A}}_i$ is given by

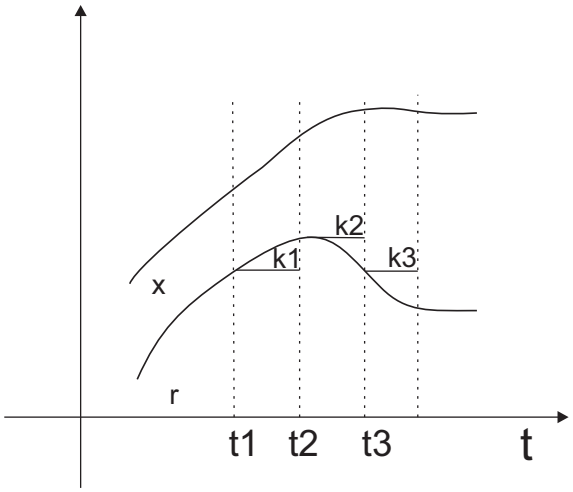

Fig. 3. Schematic computational realization of the Sample and Hold approach. Here $k_i(z) = \partial_x r(\hat{x}(z, t_i))$.

$$\sigma(\tilde{\mathcal{A}}_i) = \{\lambda_{i,n} : n \geq 1\} \tag{28}$$

and satisfies the eigenvalue problem

$$\begin{aligned} \tilde{\mathcal{A}}_{i,n}\phi_{i,n} &= \lambda_{i,n}\phi_i, \\ \tilde{\mathcal{A}}_{i,n}^*\psi_{i,n} &= \lambda_{i,n}\psi_{i,n} \end{aligned} \tag{29}$$

for all $i \in \mathbb{N}^+$ and $n \geq 1$. Furthermore, the corresponding set of eigenfunctions $\{\phi_{i,n} : n \geq 1\}$ and $\{\psi_{i,n} : n \geq 1\}$ are biorthogonal, i.e, $\langle \phi_{i,n}, \psi_{i,m} \rangle = \delta_{nm}$ and $\tilde{\mathcal{A}}_i,\ \tilde{\mathcal{A}}_i^*$ are both Riesz-spectral operators [11] which can be represented as

$$\begin{aligned} \tilde{\mathcal{A}}_{i,n} &= \sum_{n=1}^{\infty} \lambda_{i,n} \langle \cdot, \psi_{i,n} \rangle \phi_n \\ \tilde{\mathcal{A}}_{i,n}^* &= \sum_{n=1}^{\infty} \lambda_{i,n} \langle \cdot, \phi_{i,n} \rangle \psi_{i,n}. \end{aligned} \tag{30}$$

B. The Eigenvalue Problem

The operator $\tilde{\mathcal{A}}_i$ as defined in (24) is linear, but the coefficient associated to the reaction term depends on z. As a result, the calculation of its spectrum is a challenging issue. In this paper, we will consider a numerical algorithm (based on the differential transformation) to address the problem of computing the spectrum of $\tilde{\mathcal{A}}_i$ at each sampling time t_i. In particular, we will adopt the mathematical formulation proposed in [16] which is summarized as follows.

Firstly, notice that an eigenvalue $\lambda_i = \lambda(t_i)$ and its corresponding eigenvector $\phi_i(z) = \phi(z, t_i)$ should satisfy

$$\begin{aligned} \frac{1}{P_e}\frac{d^2\phi_i}{dz^2}(z) - \frac{d\phi_i}{dz}(z) - k_i(z)\phi_i(z) = \lambda_i\phi_i(z) \\ -\frac{1}{P_e}\frac{d\phi_i}{dz}(0) + \phi_i(0) = 0 \\ \frac{d\phi_i}{dz}(1) = 0. \end{aligned} \tag{31}$$

The differential transformation method, which is based on the Taylor series expansion, considers that the differential transformation $\overline{\phi_i}(k)$ and its inverse $\phi_i(z)$ are defined as

$$\overline{\phi_i}(k) = \frac{1}{k!}\frac{d^k\phi_i}{dz^k}(0), \quad \phi_i(z) = \sum_{k=0}^{\infty} z^k \overline{\phi_i}(k). \tag{32}$$

Taking the differential transformation applied to (31) yields

$$\overline{\phi}_i(k+2) = \frac{P_e}{(k+1)(k+2)}(\lambda_i\overline{\phi}_i(k) - (k+1)\overline{\phi}_i(k+1) + \sum_{l=0}^{k}\overline{k}_i(l)\overline{\phi}_i(k-l)) \tag{33}$$

$$\overline{\phi}_i(1) = P_e\overline{\phi}_i(0) \tag{34}$$

$$\sum_{k=1}^{\infty} k\overline{\phi}_i(k) = 0. \tag{35}$$

Let $\overline{\phi}_i(0) = 1$, and calculate $\overline{\phi}_i(1), ..., \overline{\phi}_i(N)$ from the recursive formula (33), where N is decided by the convergence of our design. Substituting $\overline{\phi}_i(1), ..., \overline{\phi}_i(N)$ into (35) yields

$$f_i^{(N)}(\lambda_i) = 0 \tag{36}$$

where $f_i^{(N)}(\lambda_i)$ is a Nth degree polynomial of λ_i and whose real roots are $\lambda_{i,1}, ..., \lambda_{i,N}$. Substituting $\lambda_{i,n}$ into (33) yields $\overline{\phi}_{i,n}(0), ..., \overline{\phi}_{i,n}(N)$, $\forall n = 1, ..., N$. From (32), the corresponding eigenvectors are given by

$$\phi_{i,n}(z) = \sum_{k=0}^{N} z^k \overline{\phi}_{i,n}(k). \tag{37}$$

After normalizing each $\phi_{i,n}(z)$, the sequence $\{\psi_{i,n} : n = 1, ..., N\}$ is chosen such that it is biorthonormal with the sequence $\{\phi_{i,n} : n = 1, ..., N\}$, i.e, $\langle \phi_{i,n}, \psi_{i,m} \rangle = \delta_{nm}$.

Remark 2: The methodology introduced above for the computation of the spectrum of $\tilde{\mathcal{A}}_i$ seems to be quite involved. However, the algebraic computations can be easily carried out in symbolic toolboxes of available mathematical software which will allow the online implementation of the state estimation algorithm to be described later in this section.

C. Solving the Riccati Equation

The Riccati Equation (20) for $\xi_1 = \psi_{i,n}$ and $\xi_2 = \psi_{i,m}$, with $n, m \in \mathbb{N}^+$, becomes

$$\left\langle \hat{\Pi}\psi_{i,n}, \tilde{\mathcal{A}}_i^*\psi_{i,m} \right\rangle + \left\langle \tilde{\mathcal{A}}_i^*\psi_{i,n}, \hat{\Pi}\psi_{i,m} \right\rangle - \left\langle \mathcal{C}\hat{\Pi}\psi_{i,n}, V^{-1}\mathcal{C}\hat{\Pi}\psi_{i,m} \right\rangle = 0. \tag{38}$$

If we assume that the solution has the truncated self-adjoint form

$$\hat{\Pi}_i = \sum_{n,m}^{N} \hat{\Pi}_{nm}^{(i)} \langle \cdot, \phi_{i,m} \rangle \phi_{i,n} \tag{39}$$

with $\hat{\Pi}_{nm}^{(i)} \in \mathbb{R}, \ \forall \ i, \ n, \ m \in \mathbb{N}^+$, the following holds

$$\hat{\Pi}_{nm}^{(i)} = \left\langle \psi_{i,n}, \hat{\Pi}_i\psi_{i,m} \right\rangle = \hat{\Pi}_{mn}^{(i)} = \left\langle \psi_{i,m}, \hat{\Pi}_i\psi_{i,n} \right\rangle. \tag{40}$$

Using the fact that $\lambda_{i,n}$ is an eigenvalue of the operator $\tilde{\mathcal{A}}_i^*$ and $\psi_{i,n}$ is the corresponding eigenvector, one has

$$\begin{aligned} \left\langle \hat{\Pi}_i\psi_{i,n}, \tilde{\mathcal{A}}_i^*\psi_{i,m} \right\rangle &= \left\langle \hat{\Pi}_i\psi_{i,n}, \lambda_{i,m}\psi_{i,m} \right\rangle = \lambda_{i,m}\hat{\Pi}_{nm}^{(i)} \\ \left\langle \tilde{\mathcal{A}}_i^*\psi_{i,n}, \hat{\Pi}_i\psi_{i,m} \right\rangle &= \left\langle \lambda_{i,n}\psi_{i,n}, \hat{\Pi}_i\psi_{i,m} \right\rangle = \lambda_{i,n}\hat{\Pi}_{nm}^{(i)} \end{aligned} \tag{41}$$

Notice that the representation in matrix form of (39) is given by

$$\hat{\Pi}_i = \begin{bmatrix}\phi_{i,1} \cdots \phi_{i,N}\end{bmatrix} \underbrace{\begin{bmatrix} \hat{\Pi}_{11}^{(i)} & \cdots & \hat{\Pi}_{1N}^{(i)} \\ \vdots & \ddots & \vdots \\ \hat{\Pi}_{N1}^{(i)} & \cdots & \hat{\Pi}_{NN}^{(i)} \end{bmatrix}}_{P_i} \begin{bmatrix} \langle \cdot, \phi_{i,1} \rangle \\ \vdots \\ \langle \cdot, \phi_{i,N} \rangle \end{bmatrix} \tag{42}$$

and considering the biorthogonal property of $\phi_{i,n}$ and $\psi_{i,n}$, it is straightforward to show that

$$\mathcal{C}\hat{\Pi}_i\psi_{i,n} = \underbrace{\begin{bmatrix} \langle c_1, \phi_{i,1} \rangle & \cdots & \langle c_1, \phi_{i,N} \rangle \\ \vdots & \ddots & \vdots \\ \langle c_{n_y}, \phi_{i,1} \rangle & \cdots & \langle c_{n_y}, \phi_{i,N} \rangle \end{bmatrix}}_{C} \begin{bmatrix} \hat{\Pi}_{1n} \\ \vdots \\ \hat{\Pi}_{Nn} \end{bmatrix} \tag{43}$$

likewise

$$\mathcal{C}\hat{\Pi}_i\psi_{i,m} = \underbrace{\begin{bmatrix} \langle c_1, \phi_{i,1} \rangle & \cdots & \langle c_1, \phi_{i,N} \rangle \\ \vdots & \ddots & \vdots \\ \langle c_{n_y}, \phi_{i,1} \rangle & \cdots & \langle c_{n_y}, \phi_{i,N} \rangle \end{bmatrix}}_{C} \begin{bmatrix} \hat{\Pi}_{1m} \\ \vdots \\ \hat{\Pi}_{Nm} \end{bmatrix}. \tag{44}$$

Then, regarding the term on the second row of (38), we obtain that

$$\begin{aligned} &\left\langle \mathcal{C}\hat{\Pi}_i\psi_{i,n}, V^{-1}\mathcal{C}\hat{\Pi}_i\psi_{i,m} \right\rangle \\ &\quad = \begin{bmatrix}\hat{\Pi}_{1m} & \cdots & \hat{\Pi}_{Nm}\end{bmatrix} C^T V^{-1} C \begin{bmatrix} \hat{\Pi}_{1m} \\ \vdots \\ \hat{\Pi}_{Nm} \end{bmatrix} \\ &\quad = \sum_{k,l}^{N} \mathcal{C}_{lk}\hat{\Pi}_{lm}^{(i)}\hat{\Pi}_{kn}^{(i)}. \end{aligned} \tag{45}$$

Hence, equation (38) becomes an infinite system of coupled scalar equations given by

$$(\lambda_{i,n} + \lambda_{i,m})\hat{\Pi}_{nm}^{(i)} - \sum_{k,l}^{N} \mathcal{C}_{lk}\hat{\Pi}_{lm}^{(i)}\hat{\Pi}_{kn}^{(i)} = 0, \tag{46}$$

where $\mathcal{C}_{lk}$ is the element at the l-th row and k-column of matrix $C^T V^{-1} C$.

Hence, the expression in (46) will provide $0.5N(N+1)$ coupled algebraic equations that must be solved simultaneously and may be represent in matrix form as

$$A_i P_i + P_i A_i^T - P_i C^T V^{-1} C P_i = 0 \tag{47}$$

where

$$A_i = \begin{bmatrix} \lambda_{i,1} & \cdots & 0 \\ \vdots & \ddots & \vdots \\ 0 & \cdots & \lambda_{i,N} \end{bmatrix}. \tag{48}$$

Once P_i whose entries are the parameters $\hat{\Pi}_{mn}^{(i)}$ of the self adjoint operator $\hat{\Pi}_i$ are computed by solving the algebraic Riccati equation (47), the output injection operator can be determined by means of

$$\begin{aligned} \mathcal{L}_i y &= -\hat{\Pi}_i \mathcal{C}^* V^{-1} y \\ &= -\sum_{n,m}^{N} \hat{\Pi}_{nm}^{(i)} \left\langle \mathcal{C}^* V^{-1} y, \phi_{i,m} \right\rangle \phi_{i,n} \\ &= -\sum_{n,m}^{N} \hat{\Pi}_{nm}^{(i)} \left\langle y, V^{-1} \mathcal{C} \phi_{i,m} \right\rangle \phi_{i,n} \end{aligned} \tag{49}$$

that may be represented in matrix form as

$$\mathcal{L}_i y = \begin{bmatrix} \phi_{i,1} & \cdots & \phi_{i,N} \end{bmatrix} P_i C^T V^{-1} y \tag{50}$$

D. State Estimation Algorithm

The above developments are summarized in the following state estimation algorithm for a given sampling period Δt.

EKF Algorithm:

1) **function**: Eigenspectrum(t_i, t_{i+1}) computes the sets $\{\lambda_{i,n} : n = 1, ..., N\}$, $\{\phi_{i,t} : n = 1, ..., N\}$, $\{\psi_{i,n} : n = 1, ..., N\}$ for $t \in [t_i, t_{i+1}]$ according to section III-B.
2) **function**: Riccati(t_i, t_{i+1}) solve (46) for $t \in [t_i, t_{i+1}]$.
3) **function**: Observer(t_i, t_{i+1}) solve (13) for $t \in [t_i, t_{i+1}]$ with $\hat{x}(t_0) = \hat{x}(t_i)$.
4) **input**: $\hat{x}(t_0),\ t_0$
5) **initialize**: $i = 0$
6) **while** $i \geq 0$ do
   a) $t_i = t_0 + i\Delta t$ and $t_{i+1} = t_i + \Delta t$;
   b) Output measurement: $y_i = y(t_i)$;
   c) $\tilde{\mathcal{A}}_i = \mathcal{A} + G\partial_x r(\hat{x}(t_i))\mathcal{I}$
   d) Determine the sets of eigenvalues and eigenfunctions $[\{\lambda_{i,n}\}, \{\phi_{i,n}\}, \{\psi_{i,n}\}]$=Eigenspectrum$(t_i, t_{i+1})$;
   e) Determine the solution of Riccati equation: $\hat{\Pi}_i$ =Riccati(t_i, t_{i+1});
   f) Uptade the state estimation: $\hat{x}(t_{i+1})$ =Observer(t_i, t_{i+1});
   g) $i = i + 1$.

IV. Numerical Experiments

In this section, the performance of the proposed approach is evaluated using numerical simulation of the bioreactor (1) with the numerical values taken from Table I. It is also assumed that the measured output is given by $n_y = 1$ in-domain piecewise measurement according to (6)-(7) with $\varepsilon_1 = 0.01$ and disturbed by white gaussian noise with power 4 dbW. The EKF is implemented with an initial concentration profile $\hat{x}_0(z)$ which is selected as a positive polynomial satisfying the boundary conditions and matching the initial state measurement so as to obtain a faster convergence [4]. Thus $\hat{x}_0(z)$ can be generated via the solution of the following semidefinite programming problem

$$\begin{cases} \text{Find } \hat{x}_0(z) = Z_d^T(z)\hat{Q}Z_d(z), \quad \hat{Q} > 0 \\ \quad \text{subject to} \\ \frac{1}{P_e}\partial_z \hat{x}_0(0) - \hat{x}_0(0) = -x_{in} \\ \quad \partial_z \hat{x}_0(1) = 0 \\ \quad \hat{x}_0(z_1) = x_0(z_1) \\ \quad \hat{x}_0(z) < 0.4. \end{cases} \tag{51}$$

Having selected $d = 3$, initially, the time evolution of the estimation error norm concerning the proposed state estimation scheme for different simulation scenarios were considered.

Figure 4 shows the convergence of the estimation error norm for different sensor locations considering a sampling period of $\Delta t = 0.02$, a number of modes in the eigenvalue approximation problem $N = 10$ and a variance $V = 2.5$ for implementing the EKF algorithm and generating the numerical simulation.

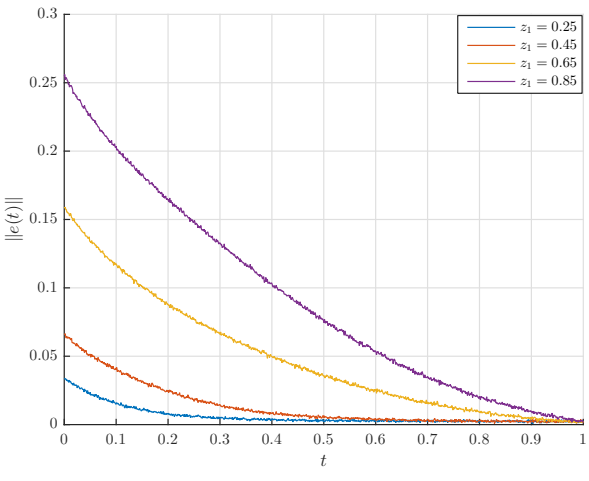

Fig. 4. Time evolution of the estimation error norm $\|e(t)\|$ for $z_1 = 0.25$, $z_1 = 0.45$, $z_1 = 0,65$, $z_1 = 0.85$.

This figure indicates that the sensor location $z_1 = 0.25$ provides the best performance with respect to other locations considered in the numerical simulation. This fact is also

supported in the minimization of the initial estimation error norm, since the initial state estimator profiles were selected to coincide with the initial measurements at the corresponding sensor locations. Moreover, this behaviour is also maintained when varying the values of V and N. Figure 5 illustrates the response for different values of V while fixing $z_1 = 0.25$ and $N = 10$, and considering the proposed EKF algorithm. It turns out that $V = 10$ becomes an appropriate estimation for the measurement noise variance among those being tested.

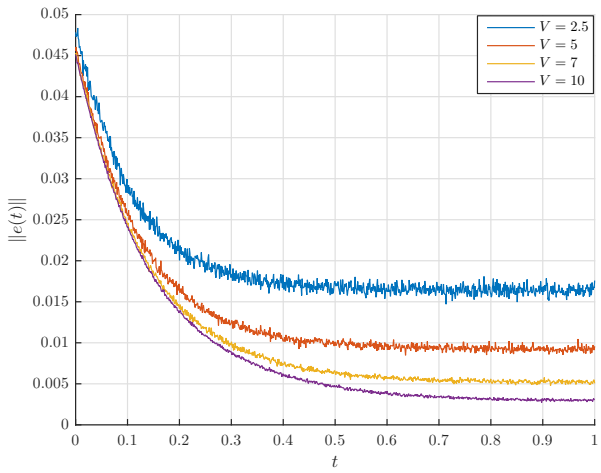

Fig. 5. Time evolution of the estimation error norm $\|e(t)\|$ for different levels of noise $V = 2.5$, $V = 5$, $V = 7$, $V = 10$.

In Figure 6, the error response is evaluated for different values of N considering $z_1 = 0.25$ and $V = 10$. It can be noticed by increasing the number of modes from $N = 5$ to $N = 15$ (considered to approximate the infinite dimensional-Riccati equation) that a similar performance is obtained. Hence, we consider $N = 10$ as an appropriate selection for the observer implementation.

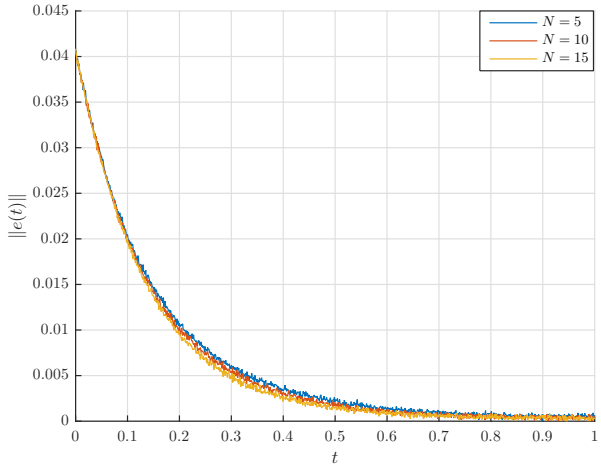

Fig. 6. Time evolution of the estimation error norm $\|e(t)\|$ for $N = 5$, $N = 10$, $N = 15$.

Then, Figure 7 shows the profile evolution of $x(z,t)$ (red lines) as well as its estimate $\hat{x}(z,t)$ (blue lines) in four different time instants and Figure 8 depicts the evolution of the estimation error surface $e(z,t)$ both considering $z_1 = 0.25$, $\Delta t = 0.02$, $N = 10$ and $V = 10$.

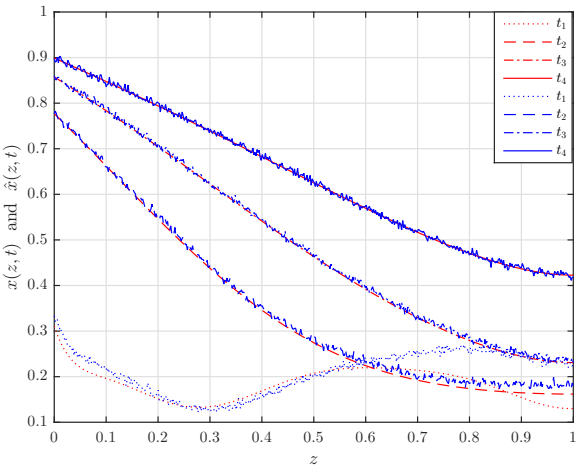

Fig. 7. Time evolution of the spatial profile of $x(z,t)$ and $\hat{x}(z,t)$ at time instants $t_1 = 1$, $t_2 = 0.25$, $t_3 = 0.5$, $t_4 = 1$

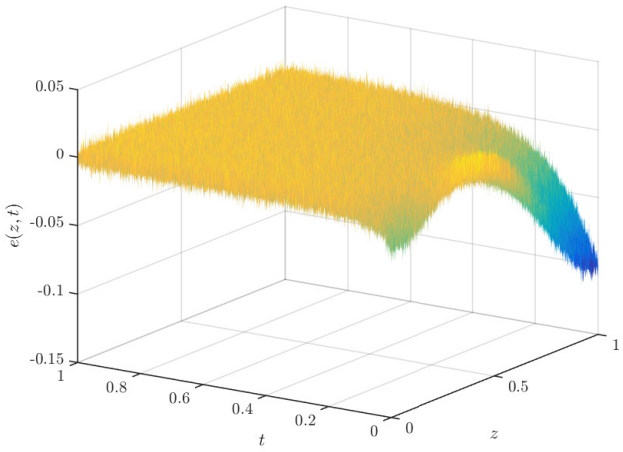

Fig. 8. Time and spatial evolution of the estimation error $e(z,t)$.

It should be observed that the procedure outlined here guarantees that the state estimate robustly converges to the true state, provided the feasibility of the solution of the Riccati equation at each sampling time for different design parameters, something that is not verifiable in advance but systematically proved from the assessment of the EKF implementation. Furthermore, as depicted in Figure 4, the sensor location influences the convergence performance of the state estimation error. Likewise, the increase of the parameter value V improves the attenuation of the measurement noise as shown in Figure 5. The decay rate convergence is slightly improved by increasing the number of modes considered in

the approximate solution of the infinite dimensional Riccati equation which is substantiated with the compensation of more slow modes presented in the error dynamics by increasing the number of terms considered in the implementation of the output injection operator defined in (50).

V. Conclusion

In this paper, an EKF-based algorithm is proposed for estimating the state of a class of semilinear PDE systems. In particular, the (extended) linearization of the semilinear estimation error system is performed around the estimated state, which results in a linear PDE system with space- and time-varying coefficients depending on the estimated state. The output injection operator is thereby systematically determined by applying a sample-and-hold approach. Herein, the spectral properties of the resulting time variant state operator are used to transform the differential Riccati equation into a set of coupled algebraic equations to be solved at each sample time. Simulation results for the simplified model of a tubular bioreactor with Monod kinetics illustrate the convergence and robustness of the state estimator regarding the discretization of the state estimator. It has been clearly noted that the proposed algorithm provides accurate estimation of the state variable provided that Δt is sufficiently small.

References

[1] I. Yupanqui Tello, A. Vande Wouver, and Daniel Coutinho. Extension of kalman filtering to semilinear pde systems-application to pulp and paper. In *2020 24th International Conference on System Theory, Control and Computing (ICSTCC)*, pages 813–818. IEEE, 2020.

[2] L. Theodore. *Chemical Reactor Analysis and Applications for the Practicing Engineer*. Wiley Online Library, 2012.

[3] A. Vande Wouwer Modeling and Simulation of Distributed Parameter Systems *Control Systems, Robotics and Automation: Modeling and System Identification-I*, page 85, 2009.

[4] A. Vande Wouwer and M. Zeitz. State estimation in distributed parameter systems. *Control Systems, Robotics and Automation–Volume XIV: Nonlinear, Distributed, and Time Delay Systems-III*, page 92, 2009.

[5] A. Vande Wouwer, C.Renotte, I. Queinnec and Ph. Bogaerts. Transient analysis of a wastewater treatment biofilter–distributed parameter modelling and state estimation. *Mathematical and computer modelling of dynamical systems*, 12(5):423-440, 2006.

[6] E. Aguilar-Garnica, J.P. García-Sandoval and C. González-Figueredo. A robust monitoring tool for distributed parameter plug flow reactors. *Computers & chemical engineering*, 35(3):510-518, 2011.

[7] A. Schaum, J.A. Moreno, E. Fridman, and J. Alvarez. Matrix inequality-based observer design for a class of distributed transport-reaction systems. *International Journal of Robust and Nonlinear Control*, 24(16):2213-2230,2014.

[8] A. Schaum, T. Meurer, and J. A. Moreno. Dissipative observers for coupled diffusion-convection-reaction systems. *Automatica*, 94:307–314, 2018.

[9] H. Dimassi, J. Winkin, and A. Vande Wouwer. A sliding mode observer for a linear reaction–convection–diffusion equation with disturbances. *Systems & Control Letters*, 124:40-48,2019.

[10] R. F. Curtain and H. Zwart. *An introduction to infinite-dimensional linear systems theory*, Springer Science & Business Media, 2012.

[11] C. Delattre, D. Dochain, and J. Winkin. Sturm-liouville systems are riesz-spectral systems. *International Journal of Applied Mathematics and Computer Science*, 13:481–484, 2003.

[12] O. Schoefs, D. Dochain, H. Fibrianto, and J.-P. Steyer. Modelling and identification of a partial differential equation model for an anaerobic wastewater treatment process. In *Proceedings of the 10th World Congress on Anaerobic Digestion, Montreal, Canada*, 1:343-347, 2004.

[13] R. F. Curtain and A. J. Pritchard. *Infinite-dimensional linear systems theory*, Springer Verlag, Berlin, 1978.

[14] M. Moarref and L. Rodrigues. Observer design for linear multi-rate sampled-data systems. In *2014 American Control Conference*, Portland, OR, USA, 2014, pp. 5319-5324.

[15] J. Winkin, D. Dochain, and P. Ligarius. Dynamical analysis of distributed parameter tubular reactors. *Automatica*, 36(3):349–361, 2000.

[16] C.-K. Chen and S.-H. Ho. Application of differential transformation to eigenvalue problems. *Applied mathematics and computation*, 79(2-3):173–188, 1996.

[17] Antonis Papachristodoulou, James Anderson, Giorgio Valmorbida, Stephen Prajna, Peter Seiler, and Pablo A Parrilo. Sum of squares optimization toolbox for matlab user's guide, 2013.